IJECBE (2025), **3**, **1**, 1–18
Received (6 July 2024) / Revised (6 July 2024)
Accepted (15 March 2025) / Published (30 May 2025)
https://doi.org/10.62146/ijecbe.v3i1.79
https://ijecbe.ui.ac.id
ISSN 3026-5258

International Journal of Electrical, Computer and Biomedical Engineering

RESEARCH ARTICLE

Economic Optimality of Automatic Generation Control in a Multi-Source Power System Using an Optimization Problem Approach

Laura Agnes Tambun and Ismi Rosyiana Fitri*

Department of Electrical Engineering, Faculty of Engineering, Universitas Indonesia, Depok, Indonesia
*Corresponding author. Email: ismi.rosyiana01@ui.ac.id

Abstract

Due to the incorporation of a high penetration of renewable energy resources into power generation, recent power system control strategies have combined economic dispatch (ED) and automatic generation control (AGC) to achieve economic operation. To this end, AGC parameters and control laws have been designed to optimize operation through the use of optimization approaches. Although existing studies indicate that the proposed AGC optimal control strategy offers superior performance compared to traditional AGC, the models used in these theoretical frameworks are typically dominated by a single energy source, such as a steam-turbine generator. Additionally, the models in existing studies do not consider the ramp generation constraints present in practical implementations. In this paper, we propose an algorithm to obtain the optimal AGC parameters to consider a more realistic power system with diverse sources. Numerical simulations are used to demonstrate the effectiveness of the proposed method.

Keywords: Economic dispatch problem (EDP), automatic generation control (AGC), adaptive participant factor, multisource, generation rate control (GRC)

1. Introduction

The operation of an electric power system has several challenges, one of them is scheduling generation units to continuously meet the load demand [1]. Additionally, the energy transition era has led Indonesia to shift its characteristics and patterns of energy use from fossil fuels to renewable energy [2]. Due to the inherent intermittent characteristic of renewable energy resources, the system may face challenges maintaining stability of frequency system. Therefore, a control mechanism is necessary to ensure that the system frequency remains within the safe limits [3].

In traditional power system, economic dispatch problem (EDP) is used to dispatch the generation output such that the total generation cost is minimized [4]. Meanwhile, automatic generation control (AGC) is utilized to regulate the system frequency to the synchronous value and maintain energy balance within each control area [5]. In light of this, with the increasing non-dispatchable resources and electric vehicles, the operator may need to allocate more reserved energy to deal with the increasing disturbance, particularly when there is a significant deviation between the actual and the forecast load. In this regard, an optimal AGC is required to maintain the system's performance while still retaining the economic aspect of system operations. In literature, studies in [6], [7], [8], [9], [10] have solved such a problem by selecting proper AGC parameters such that economic operation can be obtained. However, the model of the AGC used in [6], [7], [8] focuses on a first-order system and [9], [10] do not consider the physical limit of the generator such as ramp rate generation. To address this issue, we propose a multistage integrated ED-AGC that combines: i) a traditional economic dispatch problem (EDP), and ii) real-time AGC adjustment to obtain cost-effective generation output throughout the system operation.

Due to the need to enhance the performance of the power system in terms of economy and stability due to technical challenges arising from the use of renewable energy, numerous previous studies have focused on minimizing Economic Dispatch (ED) and Automatic Generation Control (AGC). Various approaches have been suggested to enhance the effectiveness of dynamic economic dispatch (DED). These include optimizing scheduling to balance operating costs with reliability costs as detailed in [11], and a teaching-learning algorithm that addresses a practical version of reserve-constrained dynamic economic dispatch for thermal units, accounting for network losses and operational limits of generators in [12]. In [13], a robust economic dispatch (ED) model incorporates automatic generation control (AGC) had been introduced, with an affine recourse process, optimizing both base points and participation factors of AGC units. An integrated method that merges AGC with control-based ED into a cohesive framework suitable for real-time grid operations is presented in [14]. In [15], a joint model optimizes resources for both slow timescale economic dispatch and fast timescale frequency regulation discussed. In [16], ED-AGC is split into two sub-problems: a continuous-time economic dispatch (CTED) focusing on dynamic constraints of generators and cost minimization, and an optimal automatic generation control (OAGC) aimed at minimizing generator costs while restoring frequency to its synchronous value. In [17], connecting AGC and ED by reverse engineering AGC from an optimization perspective is explored. In [18], a dynamic constrained ED model featuring AGC is proposed to ensure a more reliable and cost-effective regulation reserve schedule amidst significant net load variability.

Our main idea is to modify the traditional Economic Dispatch Problem (EDP) and adjust the parameters of the Automatic Generation Control (AGC) to ensure economic efficiency in real-time system performance. Note that optimal AGC parameters have been discussed in previous studies [6]-[10]. However, different generators may result in varying efficiency performances at different loading levels. Without proper allocation of power production across generating units, there is a risk of overburdening some generators. Therefore, this paper considers modifying the optimal AGC parameters

from an economic perspective. Specifically, we modified the objective function of the traditional EDP in [18] to include reserve cost and a quadratic penalty function. Furthermore, compared to [18], we decompose the strategy into a multistage problem to retrofit the AGC while dynamically adhering to operational constraints with AGC.

The structure of this paper is outlined as follows. Section 2 presents the fundamentals of the system such as the Traditional economic dispatch problem (EDP) and dynamic automatic generation control (AGC). This section elaborates on the decomposition problem that would be used to design the model strategy. Section 3, presents the idea and strategy of modeling the ED-AGC optimal control problem that would decomposed into two-stage problems. In section 4, we tested our proposed model with several cases to demonstrate the effectiveness of the proposed model. Finally, we summarize our findings in Section 5.

2. System and Problem Definition

This section presents the fundamentals of the Economic Dispatch Problem (EDP) and Automatic Generation Control (AGC).

2.1 Traditional EDP

The Economic Dispatch Problem (EDP) is a concept used to effectively allocate power production across generating units to minimize the total cost of generator production. Considering N generating units, let $P_{g_i}(t)$ be the dispatched power of the ith unit, and $\mathcal{N} = \{1, \ldots, N\}$. Then, the EDP is formulated as follows

$$\min_{P_{g_i}, r_i, \forall i \in \mathcal{N}} \quad \sum_{i \in \mathcal{N}} C_{g_i}(P_{g_i}) \tag{1}$$

$$\text{s.t.} \quad \sum_{i \in \mathcal{N}} P_{g_i} = P_d \tag{2}$$

$$\sum_{i \in \mathcal{N}} r_i \geq R_{req} \tag{3}$$

$$P_{g_i} + r_i \leq \overline{P_{g_i}}, \quad \forall i \in \mathcal{N} \tag{4}$$

$$P_{g_i} - r_i \geq \underline{P_{g_i}} \quad \forall i \in \mathcal{N} \tag{5}$$

where $C_{g_i}(\cdot)$ denotes the cost function for generating power. This optimization also considers several constraints, such as power balance given by (2), system-wide regulation reserve requirements in equation (3), and generator capacity limits, which account for the headroom needed for the reserve schedule enforced by (4)-(5). This concept considered the regulation reserve r_i effect that contributed potential flexibility of the power system to meet the demand. Suppose that R_{req} is the minimum requirement of the regulation reserve [18]. Note that $\underline{P_{g_i}}$ and $\overline{P_{g_i}}$ are capacity limits of the ith generating unit.

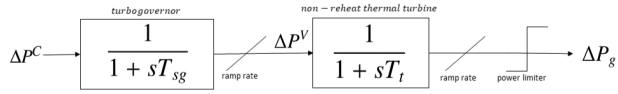

Figure 1. Dynamic response model of thermal unit-*i*

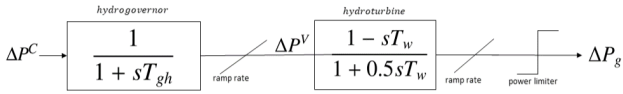

Figure 2. Dynamic response model of hydro unit-*i*.

2.2 Automatic Generation Control

This section presents the mathematical model for the design of an Automatic Generation Control (AGC) dynamic system. In this paper, a power system with only one control area is considered. Suppose that the area consists of N dispatchable generating units, AGC is aims to regulate the frequency deviation. The frequency deviation, which serves as an indicator of system stability in the event of a disturbance, is denoted by Δf. Let H and D be the inertia and damping constants, the dynamic state of frequency deviation treats load power changes ΔP_d as a disturbance, i.e.,

$$\dot{\Delta f} = \frac{1}{H}\left(\sum_{i=1}^{N} \Delta P_{g_i} - \Delta P_d - D\Delta f\right), \tag{6}$$

where ΔP_{g_i} denotes the deviation of the ith generating unit's mechanical power output. The model features a typical single-area power system, where all generators are synchronized and connected. Therefore, this system ensures that all generators exhibit a coherent response to load changes. For example, Figure 1 shows the transfer-function block diagram of the thermal generating unit. Here, T_{sg_i} and T_{t_i} represent the time constants of the governor and turbine models for the ith thermal generator. Furthermore, hydrothermal system models is illustrated in Figure 2 where T_{gh} and T_w represent the time constants of a governor and turbine for hydropower, respectively.

One can observe that Figures 1-2 includes generation-rate constraint (GRC). This can be seen as the limiter to restrict the maximum rate of valve opening or closing speed. Thus, the turbine and governor models may realistically reflect the physical limitations in adjusting the power output, contributing to more accurate and reliable AGC performance in maintaining system frequency within desired limits. In simulations, the GRC is assumed to be 0.05 [puMW] for an incremental change in the governor valve position for both thermal and hydro units. For thermal turbines, the GRC values are ±0.1/60 [puMW/s] [19]. For hydro turbines, the rising and decreasing rate values are set at 0.045 [puMW/s] and 0.06 [puMW/s], respectively [20].

In Figures 1-2, each source is modeled as a two-state dynamic system, with states corresponding to the speed governor and the turbine. For the sake of simplicity, let's initially assume that the ramp rate in the generator model can be omitted from consideration. Then, the simplified dynamic models for the governor and turbine can be written as

$$\Delta P_{g_i} = G_i^V(s)\Delta P_i^V \text{ and } \Delta P_i^V = G_i^C(s)\Delta P_i^C, \tag{7}$$

where $G_i^V(s)$ and $G_i^C(s)$ are first-order transfer-function to model the ith generating unit output in the AGC.

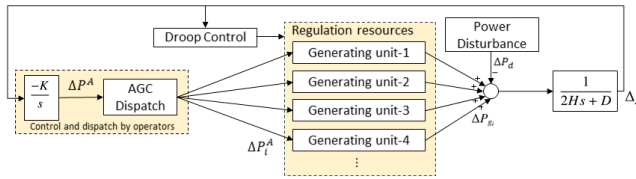

Figure 3. Load decomposition strategy

In general, the AGC refers to the secondary frequency control, which aims to regulate frequency deviations based on the inputs of the Area Control Error (ACE). Since this paper considers only a single-area control system, as illustrated in Figure 3, the AGC uses the frequency deviation as the input to the controller. Thus, together with droop control as the primary controller, ΔP_i^C can be written as:

$$\Delta P_i^C(s) = \underbrace{\frac{\Delta f(s)}{R_i}}_{\text{droop}} + \underbrace{\Delta P_i^A(s)}_{\text{AGC}}, \tag{8}$$

$$\Delta P_i^A = \alpha_i \Delta P^A,\ \alpha_i > 0,\ \sum_{i=1}^{N} \alpha_i = 1, \tag{9}$$

$$\Delta \dot{P}^A(s) = -K\Delta f, \tag{10}$$

where R_i is the droop coefficient and K is the integral feedback control gain. It is generally known that K is chosen such to regulate the frequency deviation when the system encounters disturbances from load or non-dispatchable resources variations, and to maintain operational constraints:

$$\underline{\Delta f} \le \Delta f(t) \le \overline{\Delta f},\quad \forall t \in [1, T], \tag{11}$$

where $\underline{\Delta f}$ and $\overline{\Delta f}$ are the smallest and largest frequency deviations, respectively. This implies that the system can manage minor deviations temporarily without resulting in widespread issues or power outages. Moreover, the participation factor α_i is used by operators to distribute the control signal generated by the AGC among various generating units.

2.3 Problem Definition

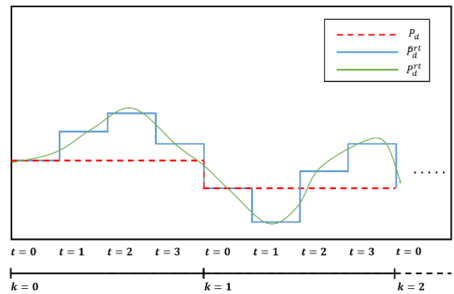

Figure 4. Load decomposition strategy

As discussed in the previous section, the EDP aims to dispatch the generation power when given the forecast load P_d. Meanwhile, the Automatic Generation Control (AGC) scheme compensates for real-time variations beyond the dispatched generator's capabilities denoted as $\Delta P_d^{rt}(t)$, $t = 0, \ldots, T-1$. In other words, the real load demand $P_d^{rt}(t)$, for all $t = 0, \ldots, T-1$, can be written as

$$P_d^{rt}(t) \quad = \quad P_d + \Delta P_d^{rt}(t). \tag{12}$$

Let a very short forecast load variation, e.g. [21], [22], can generate $\Delta \hat{P}_d^{rt}(t)$ to estimate real-time variations $\Delta P_d^{rt}(t)$, i.e., $P_d^{rt}(t) \approx \hat{P}_d^{rt}(t)$ where

$$\hat{P}_d^{rt}(t) \quad = \quad P_d + \Delta \hat{P}_d^{rt}(t). \tag{13}$$

For example, Figure 4 illustrate the given forecast demand when $T = 4$. Note that such an assumption can also be found in [**chakraborty2020dynamics**].

In practice, the time horizon for solving the Economic Dispatch Problem (EDP) can vary based on operational needs. Typically, real-time dispatch involves very short intervals, often between 5 to 15 minutes. Meanwhile, day-ahead scheduling usually spans 24 hours, divided into hourly intervals for detailed planning and coordination. Consequently, although new forecast demands $\hat{P}_d^{rt}(t)$ are obtained, it may not be practical to re-dispatch the generation P_{g_i} to respond to these variations. In light of this, we aim to ensure optimal and cost-effective power dispatch through utilizing AGC dispatch. To this end, proper α_i is chosen such that the optimal dispatch by the AGC is attained. Let $C_{r_i}(\cdot)$ be the cost function for the ith generating unit to regulate the frequency deviation. Then, we aims to minimize the total operating cost of the AGC for $t = 1, \ldots, N$, i.e.,

$$\min_{\alpha_i, i \in \mathcal{N}} \sum_{t=1}^{T} \sum_{i=1}^{N} C_{r_i}(\Delta P_i^A(t)). \tag{14}$$

The design strategy is discussed in next section.

3. Optimal AGC

This section outlined the idea and fundamental ED-AGC optimal control problem. Considering the economic perspective of AGC, we develop optimization problems to ensure cost-efficiency of the AGC operation. To incorporate the AGC model into the problem, the discrete-time model of AGC is considered.

Algorithm 1 presents the proposed method. First, the observed frequency deviation Δf_o is obtained by the operator. Then, the proposed method is a two-stage process: the first stage generated expected commands for adjusting power changes due to load deviation denoted as ΔP^A; and the second stage use the output from the first stage to solve the EDP and produce the participating factor for each generator $\alpha_i(t)$ such that the cost operation of the system is minimizes.

3.1 First Stage

One can observe that dynamic equation (6) can be discritized with sampling time T_s yields:

$$\Delta f(t+1) = \Delta f(t) + \frac{T_s}{H}\left(\sum_{i=1}^{N} \Delta P_{g_i}(t) - \Delta P_d(t) - D\Delta f(t)\right).$$

Suppose that the forecast demand $\hat{P}_d^{rt}(t)$ is also sampled every T_s. Then, substituting $\sum_{i=1}^{N} \Delta P_{g_i}(t)$ with ΔP^A yields

$$\Delta f(t+1) = \Delta f(t) + \frac{T_s}{H}\left(P^A(t) - \Delta P_d(t) - D\Delta f(t)\right), \tag{15}$$

where t denotes the sampling instant. The value $\sum_{i=1}^{N} \Delta P_{g_i}(t)$ is substituted with $P^A(t)$ since it is assumed that they are similar when ramp rate is omitted. Furthermore, equation (10) is discritized with time sampling time T_s as follows:

$$P^A(t+1) = P^A(t) - T_s K \Delta f(t). \tag{16}$$

Given the observed frequency deviation Δf_o and estimated load variation $\Delta \hat{P}_d^{rt}(t)$, consider the following optimization problem

$$\min_{P^A(t),\ t=0,\ldots,T} \quad \sum_{t=1}^{T} \frac{D}{2}\left|\Delta f(t)\right|^2$$

Problem 1: s.t. $\Delta f(0) = \Delta f_o,\ \Delta P_d(t) = \Delta \hat{P}_d^{rt}(t),$
$(11), (15), (16), \quad \forall t = 0, \ldots, T-1.$

It is important to note that in this stage, $\Delta f(t)$, $t = 1, \ldots, T$, represents the expected deviation frequency during disturbance $\Delta \hat{P}_d^{rt}(t)$. The objective of the optimization problem above primarily focuses on optimizing the quadratic penalty function, which discourages large variations in $\Delta f(t)$. However, note that we only incorporate the dynamic (15) to response of load changing $\Delta \hat{P}_d^{rt}(t)$. Note that the stability of the AGC is still maintained given that control gain K is chosen to achieve stability.

3.2 Second Stage

In order to discuss the second stage of Algorithm 1, first the dynamic of AGC in discrete-time is discussed. In this paper, GRC is incorporated in the generator model (e.g. Figures 1 and 2). Let

$$\Delta \mathsf{P} = \left[\left(\Delta P_{g_1},\, \Delta P_1^V \right), \ldots, \left(\Delta P_{g_N},\, \Delta P_N^V \right) \right]^T. \tag{17}$$

In light of this, the GRC can be generalized and written as

$$|\dot{\Delta \mathsf{P}}| \leq h_{max}, \tag{18}$$

where h_{max} is a vector with appropriate dimension. In addition, a state-variable form of dynamic equations (6)-(8) can be written as follows:

$$\underbrace{\begin{bmatrix} \dot{\Delta f} \\ \dot{\Delta \mathsf{P}} \end{bmatrix}}_{=\dot{x}} = A \underbrace{\begin{bmatrix} \Delta f \\ \Delta \mathsf{P} \end{bmatrix}}_{=:x} + B \underbrace{\begin{bmatrix} \Delta P_1^A \\ \vdots \\ \Delta P_N^A \\ \Delta P_d \end{bmatrix}}_{=:u}, \tag{19}$$

where A and B are system and control matrices with compatible dimensions. Then, the discrete-time equivalent equation of (19) is

$$x(t+1) = (1 + AT_s)x(t) + BT_s u(t), \tag{20}$$

where T_s is the sampling period and t is the sampling instant. In light of this, the GRC in (18) can be approximated with its discrete-time counterpart:

$$\left| \Delta \mathsf{P}(t+1) - \Delta \mathsf{P}(t) \right| \leq T_s h_{max}. \tag{21}$$

Given the observed frequency deviation Δf_o, the forecast load demand $\hat{P}_d^{rt}(t)$, and $\Delta P^A(t)$ from **Problem 1**, $t = 0, \ldots, T$, consider the following optimization problem

Problem 2:

$$
\begin{aligned}
\min_{P_{g_i}, r_i, \alpha_i, \forall i \in \mathcal{N}} \quad & \sum_{i=1}^{N} C_{g_i}(P_{g_i}) + \sum_{t=1}^{T} \sum_{i=1}^{N} C_{r_i}(\Delta P_i^A(t)) \\
\text{s.t.} \quad & \sum_{i \in \mathcal{N}} P_{g_i} = P_d, \\
& \sum_{i \in \mathcal{N}} r_i \geq R_{req}, \\
& P_{g_i} + r_i \leq \overline{P_{g_i}}, \qquad \forall i \in \mathcal{N}, \\
& P_{g_i} - r_i \geq \underline{P_{g_i}}, \qquad \forall i \in \mathcal{N}, \\
& \Delta P_i^A(t) = \alpha_i \Delta P^A(t), \quad \forall i \in \mathcal{N}, T = 0, \ldots, T, \\
& \sum_{i \in \mathcal{N}} \alpha_i = 1, \ \alpha_i > 0, \quad \forall i \in \mathcal{N}, \\
& \Delta f(0) = \Delta f_o, \ (11), \\
& (20) - (21), \qquad \forall t = 0, \ldots, T-1, \\
& \Delta P_d(t) = \Delta \hat{P}_d^{rt}(t), \qquad \forall t = 0, \ldots, T-1, \\
& -r_i \leq \Delta P_{g_i}(t) \leq r_i, \quad \forall i \in \mathcal{N}, t = 0, \ldots, T.
\end{aligned}
$$

The fundamental purpose of **Problem 2** is to schedule generation while ensuring cost-effectiveness of the operation of AGC. Thus, the objective function is formulated such that it minimizes the cost of dispatched power from EDP in (1) and the generating power due to frequency response $\Delta P_i^A(t)$. Since $\Delta P^A(t)$ is given from previous stage, then **Problem 2** minimizes the total cost of AGC by distributing optimal $\alpha_1, \ldots, \alpha_N$ to each generating unit. Since the GRC is omitted in (20), then (21) is incorporated to indirectly take into account the ramp rate constraints in the generator. For the sake of meeting time-variant demand, the AGC dynamic (20) response to the forecast demand $\Delta \hat{P}_d^{rt}$. Note that the reserve energy r_i plays role as power limiter for ΔP_{g_i}, i.e., $|\Delta P_{g_i}(t)| \leq r_i$. By solving Problems 1 and 2, the optimal dispatch generation and participating factor can be obtained.

The next section demonstrates that the proposed method achieves optimal AGC operation while maintaining stability.

4. Numerical Simulations

In this section, Algorithm 1 is verified using numerical simulations. The algorithm is performed for each 60-minute sampling interval. At each sampling interval, the EDP is provided with estimated load variations: $\{P_d + \Delta \hat{P}_d^{rt}(1), P_d + \Delta \hat{P}_d^{rt}(2), \ldots, P_d + \Delta \hat{P}_d^{rt}(T)\}$, with $T_s = 60$ seconds.

The CVX solver [23] was employed to solve the proposed optimization problems. The results from the solver were then dynamically integrated with the AGC model which is modeled in Matlab SIMULINK. Traditional EDP uses forecast base load for

calculating hourly dispatch generation, whereas AGC addresses the deviation load, which is derived by subtracting the real-time load from the base load.

4.1 Case and System Description

To evaluate the performance and cost-effectiveness of the proposed model, we use several study cases based on variations in load deviations and the types of generators used. The study case outlines as follows:

- **Case I**: $\Delta\hat{P}_d^{rt}(t) = \Delta P_d^{rt}(t)$. AGC consists of 5 thermal generators (5 coal-fired power plants) and one hydro power.
- **Case II**: $\Delta\hat{P}_d^{rt}(t) \neq \Delta P_d^{rt}(t)$. AGC consists of 5 thermal generators (5 coal-fired power plants) and one hydro power.

It should be noted that the estimated load deviation data $\Delta\hat{P}_d^{rt}(t)$ over 24 hours is generated through the processing of base load data using the *rand*() function in MATLAB to represent the variability of renewable energy (RE) penetration in the system. This study assumes that the maximum contribution from RE penetration is 14% of the system's base capacity. We set up the function to generate random numbers uniformly distributed within the interval (-200, 200) [MW] or equivalently (-0.14, 0.14) [p.u.]. Furthermore, the random numbers are added to the base capacity to generate the load profile with renewable energy penetration.

In this paper, the function to model the cost generation is given by [24]

$$C_{g_i} = \zeta_i + \beta_i P_{g_i} + \gamma_i P_{g_i}^2 \tag{22}$$

and

$$C_{r_i} = \mathsf{c}_i + \mathsf{b}_i P_{g_i} + \mathsf{a}_i P_{g_i}^2 \tag{23}$$

where the parameters are given in Tables 1 and 2. The model utilized five thermal generating units and one hydro-generating unit to meet the demands. Note that it is assumed that the hydro power is used only as reserve generating unit in this scenario. For the EDP, the minimum reserve requirement R_req used in this paper is 0.3 [p.u.], while the generating limits of each generator are depicted in Table 3.

Table 1. Parameters for cost function of dispatch generation $[\zeta, \beta, \gamma]$

G_1	G_2	G_3	G_4	G_5
[100, 6, 0.0003]	[200, 12, 0.0009]	[300, 18, 0.0012]	[400, 24, 0.0015]	[500, 30, 0.0015]

Depending on the type of generator, the form of the transfer function can vary, as shown in Table 4. The parameters used in the AGC system modeling include diverse time constants and droop coefficients for the governor and turbine models of both thermal and hydro generators. The generation specifications based on the test case are depicted in Table 5, with R as the primary control depicted in Table 6 [25].

In a single-area power system with multi-source generation units, we use $D = 1$ and $H = 10$ that exhibit coherent responses to load changes. The permissible Δf

Table 2. Parameters for cost of reserve generation

Case	Parameter	Generating units					
		$G1$	$G2$	$G3$	$G4$	$G5$	$G6$
		Thermal					Hydro
Case I–II	[c, b, a]	[100, 6, 0.0003]	[200, 12, 0.0006]	[300, 18, 0.0009]	[400, 24, 0.0012]	[500, 30, 0.0015]	[600, 36, 0.0018]

Table 3. Parameters for EDP

Parameter	Generating units				
	$G1$	$G2$	$G3$	$G4$	$G5$
$[\underline{P_g}, \overline{P_g}]$	[0, 0.8]	[0, 0.9]	[0, 0.8]	[0, 0.5]	[0, 1]

during the stability control response process is ±0.2 Hz. The control model of the system uses $K = 0.0967$ to manage frequency control response.

For the purpose of evaluating the optimal operation of the AGC in each case, we compared our proposed method with various combinations of α_i given in Table 7. Hydropower plants, which often function as peaker plants, have a very rapid response in adjusting power output. However, their maximum generation capacity is significantly influenced by climatic and geological conditions specific to the generation area. Additionally, these plants are often located far from demand because they require specific geographical criteria for construction [26]. Therefore, in determining the fixed alpha variation, it is assumed that the alpha value for hydro power is the smallest compared to thermal power plants.

4.2 Case I

The proposed model was tested using load variations over a 24-hour period, assuming that the actual load variations ($\Delta P_d^{rt}(t)$) are equal to the estimated load variations ($\Delta \hat{P}_d^{rt}(t)$), to assess the performance and effectiveness of the model. This load consists of estimated and real-time daily load data (24 hours or 1440 minutes) from electricity consumers in Indonesia (Figure 5). Initially in [MW], this load data was converted to per unit ([p.u.]) for analysis.

The simulation is conducted hourly, with sample data collected from the forecasted load every hour (Figure **??**) and from the real-time load every fifteen minutes (Figure **??**). The forecasted load has a peak load of 1 [p.u.] at hour 13 and a minimum load of 0.3810 [p.u.] at hour 9. Based on the real-time load, the maximum deviation requiring compensation by AGC is 0.1358 [p.u.] from minutes 1156 to 1170, and the maximum deviation from load decrease is -0.1363 [p.u.] from minutes 16 to 30.

Table 4. Transfer function of various units

Type	Transfer function
coal-fired power	$\left(\frac{1}{1+sT_{sg}}\right)\left(\frac{1}{1+sT_t}\right)$
hydro power	$\left(\frac{1}{1+sT_{gh}}\right)\left(\frac{1-sT_w}{1+0.5sT_w}\right)$
gas power	$\frac{\left(\frac{T_{gp}s+1}{T_{gq}s+1}\right)\left(\frac{T_{ag}}{T_{bg}s+T_{cg}}\right)\left(\frac{1-sT_{CR}}{1+sT_F}\right)\left(\frac{T_{kg}}{1+sT_{CD}}\right)}{1+\left(\frac{1}{R_g}\right)\left(\frac{T_{gp}s+1}{T_{gq}s+1}\right)\left(\frac{T_{ag}}{T_{bg}s+T_{cg}}\right)\left(\frac{1-sT_{CR}}{1+sT_F}\right)\left(\frac{T_{kg}}{1+sT_{CD}}\right)}$
nuclear power	$\frac{\left(\frac{1}{T_{gn}s+1}\right)\left(\frac{T_{kh}}{T_1s+1}+\frac{T_{kn}}{(T_1s+1)(T_{rh1}s+1)}+\frac{T_{rh2}s+1}{(T_{rh3}s+1)(T_2s+1)}\right)}{1+\left(\frac{1}{R_n}\right)\left(\frac{1}{T_{gn}s+1}\right)\left(\frac{T_{kh}}{T_1s+1}+\frac{T_{kn}}{(T_1s+1)(T_{rh1}s+1)}+\frac{T_{rh2}s+1}{(T_{rh3}s+1)(T_2s+1)}\right)}$

Table 5. Parameters for AGC Problem

Case	Generating units					
	$G1$	$G2$	$G3$	$G4$	$G5$	$G6$
	Thermal					Hydro
Case I–II	T_{sg}=0.08	T_{sg}=0.06	T_{sg}=0.07	T_{sg}=0.06	T_{sg}=0.06	T_{gh} = 0.2
	T_t=0.4	T_t=0.36	T_t=0.42	T_t=0.44	T_t=0.32	T_w = 1

Table 6. Droop constant for AGC Problem

Case	Generating units					
	$G1$	$G2$	$G3$	$G4$	$G5$	$G6$
	Thermal					Hydro
Case I–II	3	3	3	3.3	3	2.4

Table 7. Variations of α_i for each generator

Variation	α_1	α_2	α_3	α_4	α_5	α_6
1	$\frac{1}{6}$	$\frac{1}{6}$	$\frac{1}{6}$	$\frac{1}{6}$	$\frac{1}{6}$	$\frac{1}{6}$
2	0.2	0.3	0.1	0.1	0.2	0.1
3	0.13	0.29	0.2	0.01	0.27	0.11
4	proposed adaptive α_i					

To determine the cost-effectiveness of the proposed model, researchers compared it across various alpha variations. As shown in Table 8, the proposed model demonstrates the minimum EDP and AGC costs. The total average cost for fixed alpha variations is 1.7564e+07 Rp/[p.u.]. In comparison, the proposed model can reduce approximately 0.0085e+07 Rp/[p.u.] or about 0.4839% of the total operational costs. This indicates that the proposed model achieves significant cost-effectiveness.

The system stability response is depicted by the frequency deviation over time in Figure 7. The graph illustrates the peaks and valleys in response to disturbances. With a maximum load increase deviation, the system frequency decreases to -0.06481 Hz.

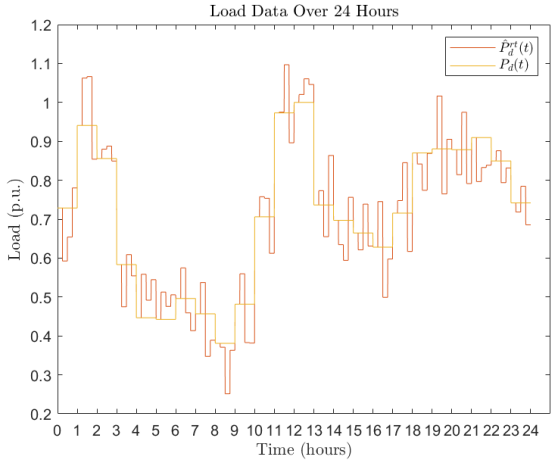

Figure 5. 24-Hour dynamic load profile case $\Delta\hat{P}d^{rt}(t) = \Delta Pd^{rt}(t)$

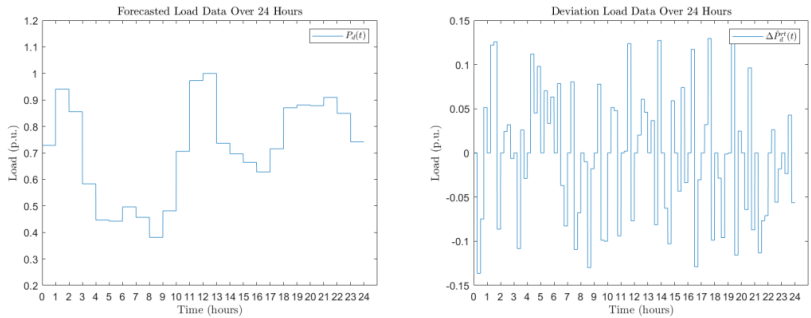

Figure 6. Decomposed load data case $\Delta\hat{P}d^{rt}(t) = \Delta Pd^{rt}(t)$: (a) Forecast load data, (b) Deviation load data

Conversely, the maximum load decrease deviation can increase the system frequency deviation up to 0.08401 Hz. Therefore, the nadir and peak points of the system frequency are 49.93519 Hz and 50.08401 Hz, respectively. Disturbances cause a sharp frequency drop, but after reaching the nadir point, the control system can recover to a stable condition without significant oscillations. The recovery time to return the frequency from the initial disturbance to nominal conditions is approximately 4 minutes. Thus, the proposed model can handle disturbances safely before the next disturbance occurs, with shorter sampling times for real-time loads compared to forecasted loads. This indicates that the model can compensate for disturbances and effectively restore stability quickly. Compared to fixed alpha frequency deviations, there are no significant differences observed with the proposed system.

Table 8. Total operational costs of case I

Variation	Total Cost
1	1.7562e+07
2	1.7565e+07
3	1.7564e+07
4	1.7479e+07

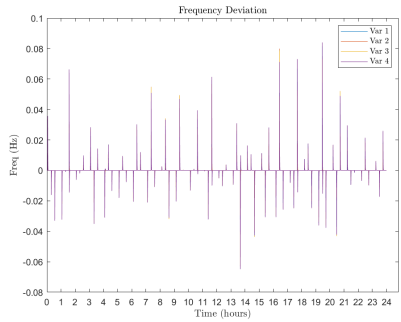

Figure 7. Frequency deviation case I

4.3 Case II

The proposed model is tested using load variations over a 24-hour period, assuming that the actual load variations ($\Delta P_d^{rt}(t)$) are not equal to the estimated load variations ($\Delta \hat{P}_d^{rt}(t)$), to assess the performance and effectiveness of the model. Forecasted load variations will be sampled every 15 minutes, while real-time load variations will be sampled every 5 minutes. This load comprises estimated and real-time daily load data (24 hours or 1440 minutes) from electricity consumers in Indonesia (Figure 8). Initially in [MW], this load data is converted to per unit ([p.u.]) for analysis.

The simulation is conducted hourly, with sample data collected from the forecasted load every hour (Figure **??**) and from the real-time load every five minutes (Figure **??**). The forecasted load has a peak load of 1 [p.u.] at hour 13 and a minimum load of 0.3810 [p.u.] at hour 9. Based on the real-time load, the maximum deviation requiring compensation by AGC is 0.1361 [p.u.] from minutes 1155 to 1160 for load increase, and the maximum deviation from load decrease is -0.1367 [p.u.] from minutes 16 to 30.

To assess the cost-effectiveness of the proposed model, researchers compared it across various alpha variations. As shown in Table 9, the proposed model demonstrates the minimum EDP and AGC costs. The total average cost for fixed alpha variations is 1.7840e+07 Rp/[p.u.]. In comparison, the proposed model can reduce approximately 0.0081e+07 Rp/[p.u.] or about 0.4540% of the total operational costs. This indicates that the proposed model achieves significant cost-effectiveness.

The system stability response is depicted by the frequency deviation over time in Figure 10. The graph illustrates the peaks and valleys in response to disturbances. With

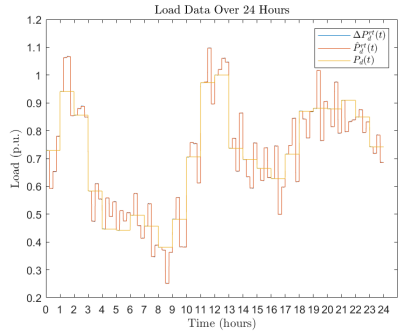

Figure 8. 24-Hour dynamic load profile case $\Delta\hat{P}_d^{rt}(t) \neq \Delta P_d^{rt}(t)$

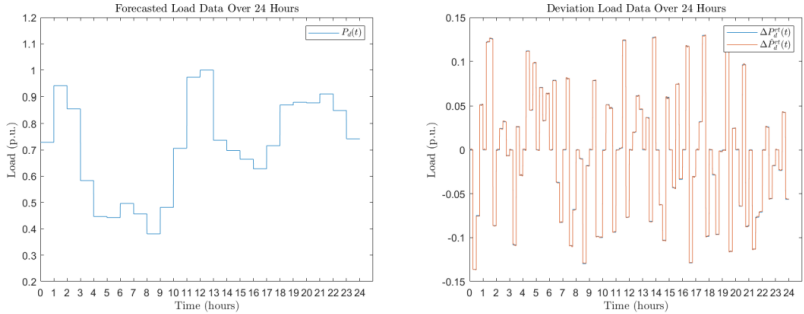

Figure 9. Decomposed load data case $\Delta\hat{P}_d^{rt}(t) \neq \Delta P_d^{rt}(t)$: (a) Forecast load data, (b) Deviation load data

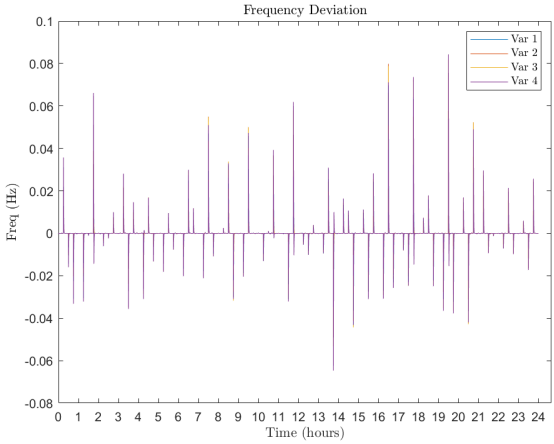

Figure 10. Frequency deviation case II

Table 9. Total operational costs of case II

Variation	Total Cost
1	1.7840e+07
2	1.7843e+07
3	1.7837e+07
4	1.7759e+07

a maximum load increase deviation, the system frequency decreases to -0.06469 Hz. Conversely, the maximum load decrease deviation can increase the system frequency deviation up to 0.08429 Hz. Therefore, the nadir and peak points of the system frequency are 49.93531 Hz and 50.08429 Hz, respectively. Disturbances cause a sharp frequency drop, but after reaching the nadir point, the control system can recover to a stable condition without significant oscillations. The recovery time to return the frequency from the initial disturbance to nominal conditions is approximately 4 minutes. Thus, the proposed model can handle disturbances safely before the next disturbance occurs, with shorter sampling times for real-time loads compared to forecasted loads. This indicates that the model can compensate for disturbances and effectively restore stability quickly. Compared to fixed alpha frequency deviations, there are no significant differences observed with the proposed system. In conclusion, the proposed model will exhibit similar stability performance to fixed alpha variations with higher cost-effectiveness.

5. Conclusion

In several experimental cases, the proposed model demonstrates the best cost-effectiveness and stability performance compared to other variations and previous research. The model reduces operational costs by approximately 0.4540%, 0.4839%, and 0.0994% compared to fixed participant factor models. The frequency response of the model reaches a minimum above 49.9 Hz with a recovery time of about 4 minutes. Despite actual load variations differing from forecasted load variations, which can cause frequency deviation fluctuations, the model effectively handles these minor differences. The stability response of the proposed model shows no significant difference when considering additional generator cost functions and adaptive participant factor concepts. Thus, the proposed model performs similarly to other variations with higher cost-effectiveness.

In the case of using identical thermal generators and non-identical ones in the AGC system, there are no significant differences in stability response. While the transient response of adaptive alpha may be slower than fixed alpha, it remains within the safe limits allowed. This is because adaptive alpha dynamically adjusts the response capabilities of each generator based on technological characteristics and model complexity while still considering operational economic aspects. This demonstrates that the proposed model remains effective and performs well in coordinating all types of backup generators to handle disturbances in the system, thereby improving operational cost-effectiveness.

References

[1] A. J. Wood, B. F. Wollenberg, and G. B. Sheble. *Power generation, operation, and control*. John Wiley & Sons, 2013.

[2] B. P. Resosudarmo, J. F. Rezki, and Y. Effendi. "Prospects of energy transition in Indonesia". In: *Bulletin of Indonesian Economic Studies* 59.2 (2023), pp. 149–177.

[3] M. Shafiullah, S. D. Ahmed, and F. A. Al-Sulaiman. "Grid integration challenges and solution strategies for solar PV systems: a review". In: *IEEE Access* 10 (2022), pp. 52233–52257.

[4] B. H. Chowdhury and S. Rahman. "A review of recent advances in economic dispatch". In: *IEEE Transactions on Power Systems* 5.4 (1990), pp. 1248–1259.

[5] F. De Mello and J. Undrill. *Automatic generation control*. 1983.

[6] R. Patel et al. "Enhancing optimal automatic generation control in a multi-area power system with diverse energy resources". In: *IEEE Transactions on Power Systems* 34.5 (2019), pp. 3465–3475.

[7] X. Zhang et al. "Bi-objective optimization of real-time AGC dispatch in a performance-based frequency regulation market". In: *CSEE Journal of Power and Energy Systems* (2020).

[8] K. Roy et al. "Regulation mileage-based generation command dispatch". In: *2023 5th International Conference on Energy, Power and Environment: Towards Flexible Green Energy Technologies (ICEPE)*. IEEE. 2023, pp. 1–6.

[9] R. Patel et al. "Optimal automatic generation control of an interconnected power system under network constraints". In: *IEEE Transactions on Industrial Electronics* 65.9 (2018), pp. 7220–7228.

[10] S. Baros, Y. C. Chen, and S. V. Dhople. "Examining the economic optimality of automatic generation control". In: *IEEE Transactions on Power Systems* 36.5 (2021), pp. 4611–4620.

[11] M. Wang et al. "Dynamic economic dispatch considering transmission–distribution coordination and automatic regulation effect". In: *IEEE Transactions on Industry Applications* 58.3 (2022), pp. 3164–3174.

[12] T. Niknam, R. Azizipanah-Abarghooee, and J. Aghaei. "A new modified teaching-learning algorithm for reserve constrained dynamic economic dispatch". In: *IEEE Transactions on Power Systems* 28.2 (2012), pp. 749–763.

[13] M. Yang et al. "Robust economic dispatch considering automatic generation control with affine recourse process". In: *International Journal of Electrical Power & Energy Systems* 81 (2016), pp. 289–298.

[14] A. T. Al-Awami. "Control-based economic dispatch augmented by AGC for operating renewable-rich power grids". In: *2019 IEEE 10th GCC Conference & Exhibition (GCC)*. IEEE. 2019, pp. 1–5.

[15] D. Cai, E. Mallada, and A. Wierman. "Distributed optimization decomposition for joint economic dispatch and frequency regulation". In: *IEEE Transactions on Power Systems* 32.6 (2017), pp. 4370–4385.

[16] P. Chakraborty et al. "Dynamics-aware continuous-time economic dispatch and optimal automatic generation control". In: *2020 American Control Conference (ACC)*. IEEE. 2020, pp. 1292–1298.

[17] N. Li, C. Zhao, and L. Chen. "Connecting automatic generation control and economic dispatch from an optimization view". In: *IEEE Transactions on Control of Network Systems* 3.3 (2015), pp. 254–264.

[18] G. Zhang, J. McCalley, and Q. Wang. "An AGC dynamics-constrained economic dispatch model". In: *IEEE Transactions on Power Systems* 34.5 (2019), pp. 3931–3940. DOI: 10.1109/TPWRS.2019.2908988.

[19] H. Sasaki et al. "A practical decentralized LFC system with generation rate limit". In: *IFAC Proceedings Volumes* 22.9 (1989). IFAC Symposium on Power Systems and Power Plant Control 1989, Seoul, Korea, 22-25 August 1989, pp. 43–48. DOI: 10.1016/S1474-6670(17)53243-7. URL: https://www.sciencedirect.com/science/article/pii/S1474667017532437.

[20] M. Khudhair et al. "Robust control of frequency variations for a multi-area power system in smart grid using a newly wild horse optimized combination of PIDD2 and PD controllers". In: *Sustainability* 14.13 (2022). DOI: 10.3390/su14138223. URL: https://www.mdpi.com/2071-1050/14/13/8223.

[21] R. Gonzalez, S. Ahmed, and M. Alamaniotis. "Implementing very-short-term forecasting of residential load demand using a deep neural network architecture". In: *Energies* 16.9 (2023), p. 3636.

[22] H. Dagdougui et al. "Neural network model for short-term and very-short-term load forecasting in district buildings". In: *Energy and Buildings* 203 (2019), p. 109408.

[23] M. Grant, S. Boyd, and Y. Ye. *CVX Users' Guide*. http://www.stanford.edu/boyd/software.html. 2009.

[24] S. Komsiyah. "Perbandingan metode Gaussian Particle Swarm Optimization (GPSO) dan Lagrange Multiplier pada masalah economic dispatch". In: *ComTech: Computer, Mathematics and Engineering Applications* 3.1 (2012), pp. 228–240.

[25] M. A. Metwally et al. "Dynamic stability analysis for Egyptian electrical grid with the first nuclear power plant". In: *Journal of Al-Azhar University Engineering Sector* 11.41 (2016), pp. 1391–1400.

[26] H. Ardiansyah. *Hydropower Technology: Potential, Challenges, and the Future*. BRIN Publishing, Jakarta, Indonesia, 2022.